AD_____

Award Number: DAMD17-02-1-0300

TITLE: Structural Basis for BRCA1 Function in Breast Cancer

PRINCIPAL INVESTIGATOR: John A. Ladias, M.D.

CONTRACTING ORGANIZATION: Beth Israel Deaconess Medical Center
Boston, MA 02215

REPORT DATE: April 2005

TYPE OF REPORT: Final

PREPARED FOR: U.S. Army Medical Research and Materiel Command
Fort Detrick, Maryland 21702-5012

DISTRIBUTION STATEMENT: Approved for Public Release;
Distribution Unlimited

The views, opinions and/or findings contained in this report are
those of the author(s) and should not be construed as an official
Department of the Army position, policy or decision unless so
designated by other documentation.

20050819098

REPORT DOCUMENTATION PAGE		*Form Approved* *OMB No. 074-0188*

Public reporting burden for this collection of information is estimated to average 1 hour per response, including the time for reviewing instructions, searching existing data sources, gathering and maintaining the data needed, and completing and reviewing this collection of information. Send comments regarding this burden estimate or any other aspect of this collection of information, including suggestions for reducing this burden to Washington Headquarters Services, Directorate for Information Operations and Reports, 1215 Jefferson Davis Highway, Suite 1204, Arlington, VA 22202-4302, and to the Office of Management and Budget, Paperwork Reduction Project (0704-0188), Washington, DC 20503

1. AGENCY USE ONLY	2. REPORT DATE April 2005	3. REPORT TYPE AND DATES COVERED Final(1 Apr 2002 – 31 Mar 2005)	
4. TITLE AND SUBTITLE Structural Basis for BRCA1 Function in Breast Cancer			**5. FUNDING NUMBERS** DAMD17-02-1-0300
6. AUTHOR(S) John A. Ladias, M.D.			

7. PERFORMING ORGANIZATION NAME(S) AND ADDRESS(ES) Beth Israel Deaconess Medical Center Boston, MA 02215 **E-Mail:** jladias@bidmc.harvard.edu	8. PERFORMING ORGANIZATION REPORT NUMBER

9. SPONSORING / MONITORING
    AGENCY NAME(S) AND ADDRESS(ES)
 	
 U.S. Army Medical Research and Materiel Command
 Fort Detrick, Maryland   21702-5012
	10. SPONSORING / MONITORING
	     AGENCY REPORT NUMBER

11. SUPPLEMENTARY NOTES

12a. DISTRIBUTION / AVAILABILITY STATEMENT Approved for Public Release; Distribution Unlimited	12b. DISTRIBUTION CODE

13. ABSTRACT (Maximum 200 Words)

The Breast Cancer Susceptibility gene 1 (BRCA1) encodes an 1863-amino acid protein that has important functions in cell cycle checkpoint control and DNA repair and plays a central role in the pathogenesis of breast cancer. Two tandem BRCA1 C-terminal domains (BRCT1 and BRCT2) are essential for the tumor suppression activity of BRAC1 and interact in a phosphorylation-dependent manner with proteins involved in DNA damage-induced checkpoint control, including the DNA helicase BACH1 and the CtBP-interacting protein (CtIP). The present project has resulted in the structure determination of the BRCA1 BRCT domains complexed with the phopshopeptide PTRVSpSPVFGAT from human CtIP (residues 322-333) at 2.5 Å resolution, using X-ray crystallography. Several hydrogen bonds and salt bridges that stabilize the BRCA1–BACH1 complex are missing in the BRCA1–CtIP interaction, offering a structural basis for the ~5-fold lower affinity of BRCA1 for CtIP than BACH1, as determined by isothermal titration calorimetry. The information obtained from these experiments has elucidated the mechanisms underlying regulation of BRCA1 by BACH1 and CtIP and has revealed the molecular changes induced by cancer-causing mutations in the BRCA1 domains that affect their interaction with these proteins.

14. SUBJECT TERMS Tumor suppressor gene, hereditary breast cancer, DNA repair, structural chemistry, X-ray crystallography			15. NUMBER OF PAGES 19
			16. PRICE CODE
17. SECURITY CLASSIFICATION OF REPORT Unclassified	18. SECURITY CLASSIFICATION OF THIS PAGE Unclassified	19. SECURITY CLASSIFICATION OF ABSTRACT Unclassified	20. LIMITATION OF ABSTRACT Unlimited

Table of Contents

INTRODUCTION

The Breast Cancer Susceptibility gene 1 (BRCA1) encodes an 1863-amino acid protein that plays a central role in the pathogenesis of hereditary breast cancer (1-3). The BRCA1 protein contains an N-terminal RING finger and two C-terminal BRCT domains (BRCT1 and BRCT2), which are critical for BRCA1-mediated tumor suppression and are targets for cancer-causing mutations (1-4). The BRCA1 RING interacts with the RING domain of BARD1, another protein involved in breast cancer pathogenesis, and with the C-terminal domain of BAP1 (amino acids 598-729), a ubiquitin hydrolase that enhances BRCA1-mediated cell growth suppression, whereas the BRCA1 BRCT domains interact with the C-terminal region of DNA helicase BACH1 (amino acids 888-1063) and the CtIP protein that contribute to the cell cycle checkpoint control and DNA repair function of BRCA1 (4-7). Importantly, it has been shown recently that the BRCA1 BRCT domains interact with phosphoserine- or phosphothreonine-containing peptides, including the BACH1(985-995) ISRTST(pS)PTFNK and CtIP(322-333) PTRVSpSPVFGAT phopshopeptides, where pS denotes phosphoserine (8-10). Moreover, a heterodimer consisting of the RING-encompassing regions of BRCA1 (amino acids 1-304) and BARD1 (amino acids 25-189) functions as a ubiquitin ligase targeting cellular proteins for destruction, whereas the individual BRCA1 and BARD1 domains have very low ubiquitin ligase activities (5). This project focuses on the elucidation of the structural basis of the BRCA1 RING and BRCT domains interaction with BARD1, BAP1, BACH1, and CtIP, using X-ray crystallography. Because BRCA1 plays a central role in breast cancer pathogenesis, the determination of its three-dimensional structure will facilitate the unraveling of the molecular mechanisms of its function in breast carcinogenesis. The Specific Aims of this proposal are:

Specific Aim 1. To co-crystallize and determine the crystal structure of the BRCA1 RING (amino acids 1-103) bound to the C-terminal domain of BAP1 (amino acids 598-729).

Specific Aim 2. To determine the crystal structure of the ubiquitin ligase heterodimer consisting of the BRCA1 region spanning amino acids 1-304 and the BARD1 region spanning residues 25-189.

Specific Aim 3. To co-crystallize and determine the crystal structure of the BRCA1 BRCT1/BRCT2-containing region (amino acids 1646-1859) complexed with the BACH1 and CtIP phosphopeptides.

BODY

During the award period we proceeded with the completion of the experiments proposed in Task 2 of the revised Statement of Work (as described in the first year's progress report). A description of our progress in these studies follows below.

Task 2a. To clone the BRCA1 BRCT1/BRCT2-containing region (residues 1646-1859), the BAP1 C-terminal domain (residues 598-729), and the BACH1 region (residues 888-1063) into prokaryotic expression vectors for production in *E. coli* cells (months 13-16). The DNA fragment encoding the human BRCA1 BRCT1/BRCT2 domain (amino acids 1646-1859) was amplified with the polymerase chain reaction (PCR) using the human BRCA1 cDNA as a template and cloned into a modified pTYB12 prokaryotic vector (New England BioLabs), following standard protocols (11). The resulting construct was verified by DNA sequencing and was used to transform *E. coli* ER2566 cells (NEB).
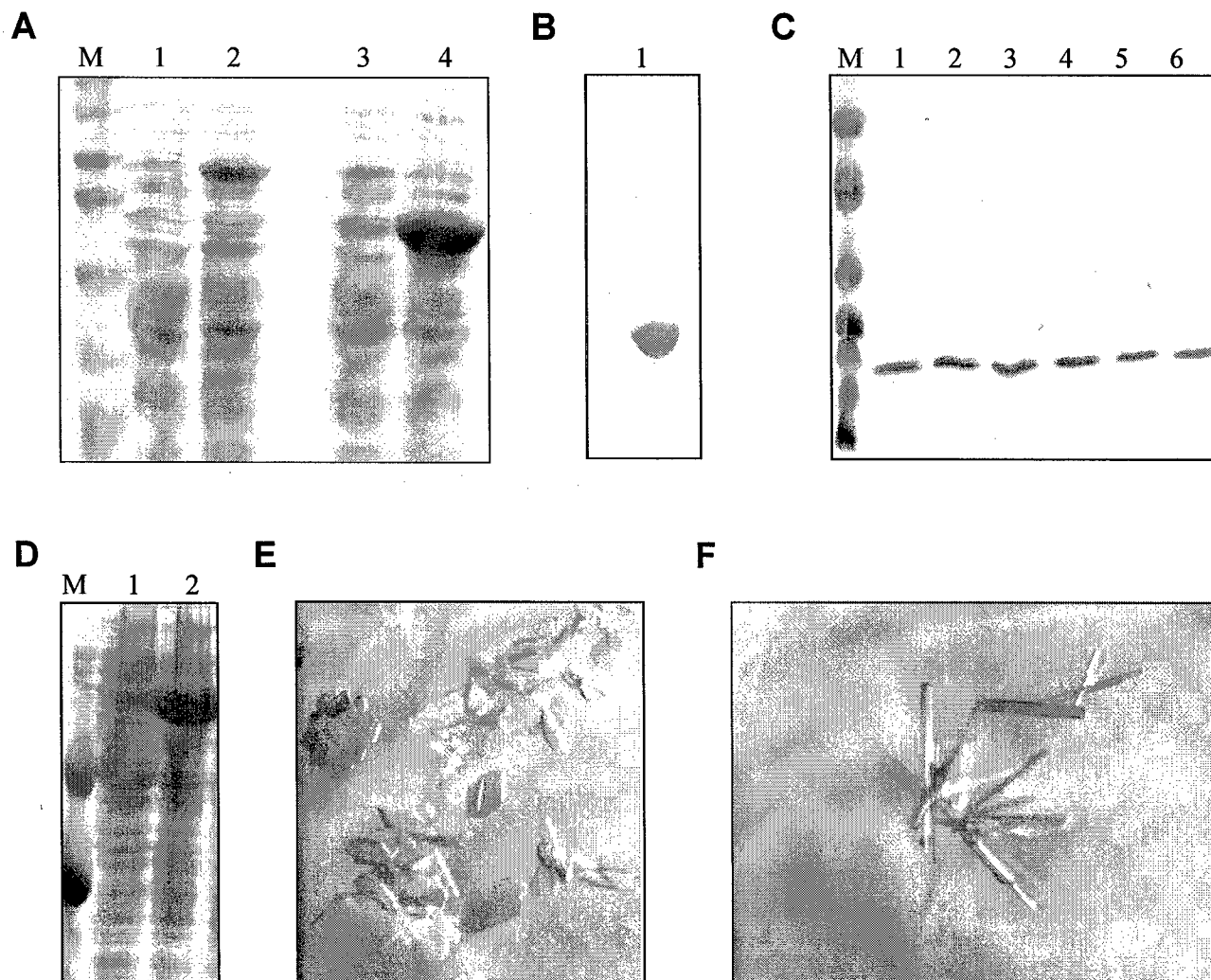
4

Figure 1. (A) Expression of the BRCA1 BRCT1/BRCT2 domain (amino acids 1646-1859) and the BAP1 C-terminal domain (amino acids 598-729). SDS-PAGE of intein-BRCT1/BRCT2 and intein-BAP1 fusion proteins produced in *E. coli* cells. *Lane M*: protein markers; *lanes 1 and 2*: uninduced and induced whole-cell extracts, respectively, of *E. coli* ER2566 cells expressing intein-BRCT1/BRCT2 protein; *lanes 3 and 4*: uninduced and induced whole-cell extracts, respectively, of *E. coli* cells expressing intein-BAP1(598-729) protein. **(B)** Purified BRCT1/BRCT2(1646-1859) protein following overnight cleavage from intein with DTT at 4°C and concentration. **(C)** *Lane M*: protein markers; *lanes 1-6*: eluted fractions of purified BAP1(598-729) protein following overnight cleavage from intein with DTT at 4°C. **(D)** Expression of the BACH1 domain (residues 888-1063). SDS-PAGE of intein-BACH1 fusion protein produced in *E. coli* ER2566 cells. *Lane M*: protein markers; *lanes 1 and 2*: uninduced and induced whole-cell extracts, respectively, of *E. coli* cells expressing intein-BACH1 protein. **(E)** Microcrystalline plates of recombinant BRCA1 RING protein (residues 1-103) bound to BAP1 C-terminal domain (amino acids 598-729), grown using the sitting drop vapor diffusion method. **(F)** Needle-like crystals of the BRCA1 BRCT1/BRCT2 domain (amino acids 1646-1859) bound to the BACH1 phosphoserine-containing peptide ISRTST(pS)PTFNK, grown using the sitting drop vapor diffusion method.

5

To clone the C-terminal domain of human BAP1 we obtained the cDNA KIAA0272 from Dr. Takahiro Nagase at the Kazusa DNA Research Institute, Japan, which codes for the human BAP1 protein (accession number D87462). Using this cDNA as a template, we amplified by PCR a DNA fragment encoding the BAP1 C-terminal domain (residues 598-729) and cloned it into a modified pTYB12 prokaryotic vector, using standard methods. The resulting construct was verified by DNA sequencing and was used to transform *E. coli* ER2566 cells (NEB).

Several requests to obtain the human BACH1 cDNA from other laboratories were denied, so we proceeded with cloning the DNA fragment coding for the BACH1 region (residues 888-1063) from a human brain cDNA library (Clontech) using PCR. The obtained DNA fragment was cloned into a modified pTYB12 prokaryotic vector. The resulting construct was verified by DNA sequencing and was used to transform *E. coli* ER2566 cells (NEB).

Task 2b. To express the BRCA1 BRCT1/BRCT2-containing region (residues 1646-1859), the BAP1 C-terminal domain (residues 598-729), and the BACH1 region (residues 888-1063) in *E. coli* cells (months 17-24).

The BRCA1 BRCT1/BRCT2 protein was produced in ER2566 cells as a fusion with intein. Expression of the fusion protein was induced at 20°C by 1 mM IPTG at OD_{600} of 0.6 (Figure 1A, lanes 1,2), purified on chitin beads (NEB) using the manufacturer's protocols, was further purified by size-exclusion chromatography and was concentrated using Centriprep concentrators (Amicon) for use in crystallization experiments (Figure 1B), as we described previously (12-17).

For the production of the BAP1(598-729) recombinant protein, we followed a similar approach. Briefly, expression of the BAP1(598-729) protein as a fusion with intein in ER2566 cells was induced at 20°C by 1 mM IPTG at OD_{600} of 0.6 (Figure 1A, lanes 3,4), purified on chitin beads (NEB) using the manufacturer's protocols (Figure 1C), was further purified by size-exclusion chromatography and was concentrated using Centriprep concentrators for use in crystallization experiments, as we described previously (12-17).

The recombinant protein BACH1(888-1063) was produced in ER2566 cells as a fusion with intein following a similar strategy. Expression of the fusion protein was induced at 22°C by 1 mM IPTG at OD_{600} of 0.6 (Figure 1D, lanes 1,2), purified on chitin beads (NEB) using the manufacturer's protocols, was further purified by gel filtration and was concentrated using Centriprep concentrators for use in crystallization trials, as we described previously (12-17). In general, using this expression system we were able to obtain up to 5-7 mg of recombinant protein (>98% pure as estimated by SDS-PAGE) per liter of bacterial culture.

Task 2c. To crystallize the BRCA1 BRCT1/BRCT2(1646-1859) in complex with BACH1 and CtIP phosphopeptides, and the BRCA1(1-103) in complex with BAP1(598-729), using sparse matrix vapor diffusion crystallization methods, seeding, limited proteolysis, and mutagenesis to improve crystallization (months 18-24).

Having purified these proteins to near homogeneity, we proceeded with crystallization experiments. The protein complexes BRCA1(1646-1859)–BACH1(888-1063), BRCA1(1-103)–BAP1(598-729), and BRCA1(1646-1859)–BACH1(984-995) phosphopeptide, were formed by mixing the corresponding proteins at stoichiometric ratios, followed by purification of the complexed proteins by gel filtration. Subsequently, the protein complexes were concentrated and used for crystallization experiments, as described in the original application. To date, the protein complex BRCA1(1646-1859)–BACH1(888-1063) did not yied any crystals. By contrast, small crystals were obtained with the BRCA1(1-103)–BAP1(598-729) complex (Figure 1E), and the

BRCA1(1646-1859)–BACH1(984-995) phosphopeptide complex (Figure 1F). Currently we are in the process of optimizing the crystallization conditions in order to obtain large single crystals of these complexes that diffract to high resolution and determine the structures of these proteins. Because the BRCA1 BRCT bound to BACH1 phosphopeptide structure has been published by other groups we initiated structural studies of the BRCT-CtIP complex. The BRCA1 BRCT domains interact with the CtIP protein forming a complex that is required for the DNA damage-induced cell cycle checkpoint control. This interaction depends on the phosphorylation of serine 327 of CtIP and its disruption allows cells with damaged DNA to enter the next cell cycle phase without proper DNA repair, leading subsequently to genomic instability.
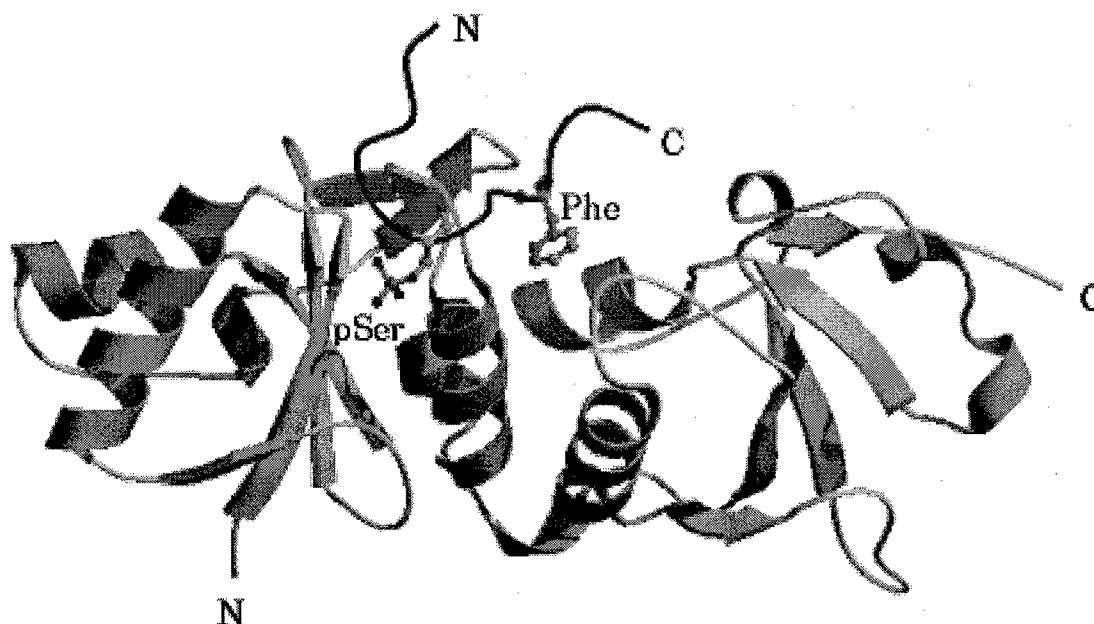

Figure 2. Ribbons representation of the BRCA1 BRCT domains bound to CtIP phosphopeptide. The critical residues pSer 0 and Phe +3 are denoted.

The bacterially produced purified BRCA1 BRCT domains were co-crystallized with the peptide PTRVSpSPVFGAT (pS denoting phosphorylated serine) corresponding to amino acid residues 322-333 of human CtIP. The crystal structure was determined at 2.5 Å resolution using synchrotron radiation. The peptide interacts with the BRCT domains in a two-pronged manner, with the phosphorylated serine 327 and phenylalanine 330 anchoring the peptide through extensive contacts with BRCA1 residues (Figure 2). The structure also shows that the cancer-associated mutation M1775R causes steric hiderance with phenylalanine 330 that disrupts the BRCA1-CtIP interaction. The crystal structure of the BRCA1 BRCT-CtIP complex reveals the molecular determinants underlying the specificity and affinity of this dynamic interaction that is critical for DNA damage-induced cell cycle checkpoint control, and it provides a structural basis to explain the detrimental effects of certain tumor-associated BRCA1 mutations on this interaction. A manuscript describing this work has been submitted for publication (*attached*).

KEY RESEARCH ACCOMPLISHMENTS

1. Cloning of the BRCA1 BRCT1/BRCT2-containing region (residues 1646-1859) into a modified pTYB12 prokaryotic expression vector for production in *E. coli* cells (*Task 2a*).
2. Cloning of the BAP1 C-terminal domain (residues 598-729) into a modified pTYB12 prokaryotic expression vector for production in *E. coli* cells (*Task 2a*).
3. Cloning of the BACH1 region (residues 888-1063) into a modified pTYB12 prokaryotic expression vector for production in *E. coli* cells (*Task 2a*).
4. Expression of the BRCA1 BRCT1/BRCT2 (residues 1646-1859) in *E. coli* ER2566 cells and purification of the recombinant protein using chromatographic methods (*Task 2b*).
5. Expression of the BAP1 C-terminal domain (residues 598-729) in *E. coli* ER2566 cells and purification of the recombinant protein using chromatographic methods (*Task 2b*).
6. Expression of the BACH1 region (residues 888-1063) in *E. coli* ER2566 cells and purification of the recombinant protein using chromatographic methods (*Task 2b*).
7. Crystallization experiments of the BRCA1 BRCT1/BRCT2(1646-1859) protein bound to BACH1(888-1063) protein using sparse matrix vapor diffusion crystallization methods, so far producing no crystals (*Task 2c*).
8. Crystallization experiments of the BRCA1 BRCT1/BRCT2(1646-1859) protein bound to the BACH1(985-995) phosphopeptide ISRST(pS)PTFNK using sparse matrix vapor diffusion crystallization methods, resulting in small crystalline plates (*Task 2c*).
9. Crystallization experiments of the BRCA1 RING(1-103) protein bound to BAP1 C-terminal domain (residues 598-729) using sparse matrix vapor diffusion crystallization methods, resulting in small needle-like crystals (*Task 2c*).
10. Crystallization experiments of the BRCA1 BRCT1/BRCT2(1646-1859) protein bound to the CtIP(322-333) phopshopeptide PTRVSpSPVFGAT using sparse matrix vapor diffusion crystallization methods, resulting in high-quality crystals (*Task 2c*).
11. Crystal structure determination of the BRCT1/BRCT2(1646-1859) protein bound to the CtIP(322-333) phopshopeptide PTRVSpSPVFGAT at 2.5 Å resolution using synchrotron radiation (*Tasks 2c and 3f*).

REPORTABLE OUTCOMES

The experiments of this project are still in progress and no new publications have resulted so far. A manuscript describing the BRCA1-CtIP crystal structure has been submitted for publication (*attached*).

CONCLUSIONS

During the award period we completed the Tasks 2a, 2b, and 2c of the revised Statement of Work. In addition, the recent discovery that the BRCA1 BRCT1/BRCT2 domains interact with phosphoserine- or phosphothreonine-containing peptides, including the BACH1(985-995) ISRTST(pS)PTFNK and CtIP(322-333) PTRVSpSPVFGAT phopshopeptides (8-10), provided a compelling reason for us to initiate crystallization experiments of these domains complexed with this peptide, a task that was not included in the original Statement of Work. The crystal structure

of BRCA1 BRCT1/BRCT2 domains bound to the target phosphopeptides will provide much more information than the structures of these domains in the unbound form (18). The information obtained from these experiments will elucidate the mechanisms underlying regulation of BRCA1 by BAP1, BACH1, and CtIP and will reveal the molecular changes induced by cancer-causing mutations in the BRCA1 domains that affect their interaction with BAP1, BACH1, and CtIP. A manuscript describing the BRCA1-CtIP crystal structure has been submitted for publication (*attached*).

I would like to emphasize that although the award period is finished, we will continue to pursue very persistently the crystallographic analysis of the BRCA1 BRCT and RING domains, as outlined in the original proposal. The Idea Award has provided critical support to initiate this research project and the successful completion of these studies will be reported to DOD in the future.

REFERENCES

1. Venkitaraman AR. (2002). Cancer susceptibility and the functions of BRCA1 and BRCA2. *Cell* **108**: 171-182
2. Scully R, Livingston DM. (2000). In search of the tumour-suppressor functions of BRCA1 and BRCA2. *Nature* **408**: 429-432
3. Welcsh PL, Owens KN, King MC. (2000). Insights into the functions of BRCA1 and BRCA2. *Trends Genet.* **16**: 69-74
4. Deng CX, Brodie SG. (2000). Roles of BRCA1 and its interacting proteins. *Bioessays* **22**: 728-737
5. Hashizume R, Fukuda M, Maeda I, Nishikawa H, Oyake D, Yabuki Y, Ogata H, Ohta T. (2001). The RING heterodimer BRCA1-BARD1 is a ubiquitin ligase inactivated by a breast cancer-derived mutation. *J. Biol. Chem.* **276**: 14537-14540
6. Jensen DE, Proctor M, Marquis ST, Gardner HP, Ha SI, Chodosh LA, Ishov AM, Tommerup N, Vissing H, Sekido Y, Minna J, Borodovsky A, Schultz DC, Wilkinson KD, Maul GG, Barlev N, Berger SL, Prendergast GC, Rauscher FJ. (1998). BAP1: a novel ubiquitin hydrolase which binds to the BRCA1 RING finger and enhances BRCA1-mediated cell growth suppression. *Oncogene* **16**: 1097-1112
7. Cantor SB, Bell DW, Ganesan S, Kass EM, Drapkin R, Grossman S, Wahrer DC, Sgroi DC, Lane WS, Haber DA, Livingston DM. (2001). BACH1, a novel helicase-like protein, interacts directly with BRCA1 and contributes to its DNA repair function. *Cell* **105**: 149-160
8. Yu X, Chini CC, He M, Mer G, Chen J. (2003). The BRCT domain is a phospho-protein binding domain. *Science* **302**: 639-642
9. Manke IA, Lowery DM, Nguyen A, Yaffe MB. (2003). BRCT repeats as phosphopeptide-binding modules involved in protein targeting. *Science* **302**: 636-639
10. Rodriguez M, Yu X, Chen J, Songyang Z. (2003). Phosphopeptide binding specificities of BRCA1 COOH-terminal (BRCT) domains. *J. Biol. Chem.* **278**: 52914-52918
11. Sambrook J, Fritsch EF, Maniatis T. (1989). Molecular Cloning: A Laboratory Manual (Cold Spring Harbor, New York: Cold Spring Harbor Laboratory Press)

12. Hiremath CN, Ladias JAA. (1998). Expression and purification of recombinant hRPABC25, hRPABC17, and hRPABC14.4, three essential subunits of human RNA polymerases I, II, and III. *Prot. Expr. Purif.* **13:** 198-294

13. Webster G, Leung T, Karthikeyan S, Birrane G, Ladias JAA. (2001). Crystallographic characterization of the PDZ1 domain of the Na^+/H^+ exchanger regulatory factor. *Acta Crystallogr.* **D57:** 714-716

14. Karthikeyan S, Leung T, Birrane G, Webster G, Ladias JAA. (2001). Crystal structure of the PDZ1 domain of the human Na^+/H^+ exchanger regulatory factor provides insights into the mechanism of carboxyl-terminal leucine recognition by class I PDZ domains. *J. Mol. Biol.* **308:** 963-973

15. Karthikeyan S, Leung T, Ladias JAA. (2001). Structural basis of the Na^+/H^+ exchanger regulatory factor PDZ1 interaction with the carboxyl-terminal region of the cystic fibrosis transmembrane conductance regulator. *J. Biol. Chem.* **276:** 19683-19686

16. Karthikeyan S, Leung T, Ladias JAA. (2002). Structural Determinants of the Na^+/H^+ exchanger regulatory factor interaction with the β_2 adrenergic and platelet-derived growth factor receptors. *J. Biol. Chem.* **277:** 18973-18978

17. Birrane G, Chung J, Ladias JAA. (2003). Novel Mode of Ligand Recognition by the Erbin PDZ Domain. *J. Biol. Chem.* **278:** 1399-1402

18. Williams RS, Green R, Glover JN. (2001). Crystal structure of the BRCT repeat region from the breast cancer-associated protein BRCA1. *Nat. Struct. Biol.* **8:** 838-842

Structural Basis for Cell Cycle Checkpoint Control by the BRCA1-CtIP Complex

Ashok K. Varma, Raymond S. Brown, Gabriel Birrane, and John A.A. Ladias*

Molecular Medicine Laboratory and Macromolecular Crystallography Unit, Division of Experimental Medicine, Harvard Institutes of Medicine, Harvard Medical School, Boston Massachusetts 02115

Address correspondence to: John A.A. Ladias, Harvard Institutes of Medicine, Room 354, 4 Blackfan Circle, Boston MA 02115; Tel: 617-667-0064; Fax: 617-975-5241; E-mail: jladias@bidmc.harvard.edu

The breast and ovarian tumor suppressor BRCA1 has important functions in cell cycle checkpoint control and DNA repair. Two tandem BRCA1 C-terminal (BRCT) domains are essential for the tumor suppression activity of BRAC1 and interact in a phosphorylation-dependent manner with proteins involved in DNA damage-induced checkpoint control, including the DNA helicase BACH1 and the CtBP-interacting protein (CtIP). The crystal structure of the BRCA1 BRCT repeats bound to the phosphopeptide PTRVSpSPVFGAT corresponding to residues 322-333 of human CtIP was determined at 2.5 Å resolution. The peptide binds to a cleft formed by the interface of the two BRCTs in a two-pronged manner, with the phospho-Ser327 and Phe330 anchoring the peptide through extensive contacts with BRCA1 residues. Several hydrogen bonds and salt bridges that stabilize the BRCA1–BACH1 complex are missing in the BRCA1–CtIP interaction, offering a structural basis for the ~5-fold lower affinity of BRCA1 for CtIP than BACH1, as determined by isothermal titration calorimetry. Importantly, the side chain of Arg1775 in the cancer-associated BRCA1 mutation M1775R sterically clashes with the phenyl ring of CtIP Phe330 disrupting the BRCA1–CtIP interaction. These results provide new insights into the molecular mechanisms underlying the dynamic selection of target proteins involved in DNA repair and cell cycle control by BRCA1 and reveal how certain cancer-associated mutations affect these interactions.

The breast and ovarian cancer susceptibility gene *BRCA1* encodes a 1,863-residue multifunctional protein that participates in genomic stability maintenance through its function in the repair of double-strand DNA breaks (DSBs), cell cycle checkpoint control, protein ubiquitination, and transcriptional regulation (1–3). *BRCA1* functions as a tumor suppressor and germline mutations in this gene are associated with a high incidence of familial breast and ovarian cancer (1, 2). The BRCA1 protein contains two BRCT domains that are frequent targets of cancer-causing mutations. In fact, the majority of clinically validated *BRCA1* mutations produce truncated BRCA1 polypeptides that lack one or both BRCT repeats and several missense mutations that affect the structure of these domains are associated with early-onset breast and ovarian cancer (2, 4). These findings, together with the observation that genetic deletion of the BRCA1 BRCT domains leads to tumor development in mice (5), demonstrate that the structural integrity of these modules is essential for the tumor suppressor activity of BRCA1.

Although the mechanisms underlying tumor suppression by BRCA1 remain largely unknown, mounting evidence indicates that the interaction of the BRCT domains with proteins involved in DNA damage-induced cell cycle checkpoint control and DNA repair plays a key role in this function (1–3). In response to genotoxic insults, such as ionizing radiation, BRCA1 is phosphorylated by the ATM kinase and localizes at DNA damage sites, where it is thought to participate in the assembly of DNA repair complexes. BRCA1 is an essential

1

component of the DNA damage-induced S-phase and G2/M-phase checkpoints (6), and BRCA1-deficient cells exhibit defects in homology-directed DNA repair, being hypersensitive to ionizing radiation and agents that crosslink DNA strands or produce DSBs, such as cisplatin and mitomycin C (7–10). BRCA1 BRCT binding to the DNA helicase BACH1 (11) and the transcriptional co-repressor CtIP (12–14) plays a central role in the G2/M checkpoint control (15, 16). Recent studies have demonstrated that the BRCA1 BRCT repeats are phosphoprotein-binding modules (17–19) and have shown that phosphorylation of the BACH1 and CtIP proteins at Ser990 and Ser327, respectively, is essential for recognition by these domains (16, 18, 19). CtIP was originally identified as a binding partner of the transcriptional corepressor CtBP (12), and was subsequently shown to interact with and mediate transcriptional repression by the retinoblastoma (pRB) tumor suppressor and the pRB-related protein p130 (20). Importantly, CtIP is phosphorylated on Ser327 only in G2-phase and controls the G2/M transition checkpoint through its transient interaction with the BRCA1 BRCT repeats, which differs from the more stable BRCA1–BACH1 association that persists in the S-through M-phase and controls the G2 accumulation checkpoint (16, 18, 19).

Recent crystal and solution structures of the BRCA1 BRCT domains bound to BACH1 and artificial phosphopeptides have offered mechanistic insights into ligand recognition by these modules (21–24). The BACH1 peptide inserts in a conserved surface cleft at the junction of the two BRCT domains, with phospho-Ser990 and Phe993 of BACH1 providing the main interactions with BRCA1 residues. To further elucidate the specificity and affinity determinants of BRCT–ligand interactions, we determined the crystal structure of the BRCA1 BRCT repeats bound to a CtIP phosphopeptide. As in the BRCA1–BACH1 structures (21, 22), the CtIP phospho-Ser327 and Phe330 anchor the peptide to the conserved BRCT cleft. However, several hydrogen bonds and salt bridges that stabilize the BRCA1–BACH1 interaction are missing in the BRCA1–CtIP complex, providing a structural explanation for the lower affinity and transient nature of the BRCA1 association with CtIP as compared to BACH1.

EXPERIMENTAL PROCEDURES

Protein Purification and Crystallization— The human BRCA1 BRCT protein (residues 1646–1859) was expressed in *Escherichia coli* BL21(DE3) cells as a glutathione *S*-transferase fusion, purified on glutathione Sepharose, released with thrombin digestion, and further purified on a Superdex 75 column (Amersham Biosciences). The BRCT protein (25 mg/ml in phosphate-buffered saline, pH 7.4, supplemented with 300 mM NaCl) was mixed with the synthetic phosphopeptide PTRVSpSPVFGAT (pS denoting phosphoserine) at 1:1.5 molar ratio and was crystallized by the sitting drop vapor diffusion method at 20°C with addition of 1.75 M ammonium sulfate, 0.1 M MES, pH 6.7, 10 mM cobalt chloride. Crystals were cryoprotected in mother liquor containing 25% glycerol and were flash-frozen in liquid nitrogen. Diffraction data were collected on beamline X12B at the National Synchrotron Light Source, Brookhaven National Laboratory, Long Island, New York. The crystals belong to space group $P6_122$ with unit cell dimensions $a = b = 113.1$ Å, $c = 121.9$ Å, $\alpha = \beta = 90°$, $\gamma = 120°$. The data were reduced and merged using the programs DENZO and SCALEPACK (25) (Table 1).

Structure Determination and Refinement— The BRCT–CtIP structure was determined by molecular replacement using PHASER (26) and the BRCA1 BRCT–BACH1 structure (PDB 1T15) with the BACH1 peptide removed, as the search model. Refinement with CCP4 (27) and REFMAC5 (28) produced initial $2F_o - F_c$ and $F_o - F_c$ maps with contiguous electron density for the CtIP peptide. The molecular geometry of the structure was improved with CNS (29) and by manual model building using O (30). Water molecules were found with ARP/wARP (31). The final model contains 1,786 protein atoms, 48 water molecules, one sulfate ion and one cobalt ion. The crystallized BRCT protein includes the vector-derived residues GS at its N terminus.

Isothermal Titration Calorimetry—Binding constants of the BRCA1 BRCT domains to the BACH1 and CtIP phosphopeptides were measured using a VP-ITC microcalorimeter (MicroCal). Briefly, 0.1323 mM of the BACH1 peptide ISRSTpSPTFNKQ and 0.2096 mM of the CtIP peptide PTRVSpSPVFGAT were titrated against a

0.0188 mM solution of BRCA1 BRCT protein in phosphate-buffered saline, 300 mM NaCl, at 25°C. Titration curves were analyzed using the program ORIGIN 5.0 (OriginLab).

RESULTS AND DISCUSSION

CtIP Phosphopeptide Recognition by the BRCA1 BRCT Domains—As described previously (21–24), the BRCA1 region spanning residues 1646–1859 folds into two tandem domains (BRCT1 and BRCT2), each comprising a central β-sheet formed by four parallel β-strands (β1 to β4) and flanked by two α-helices (α1 and α3) on one side and a single α-helix (α2) on the other (Fig. 1*A*). The two BRCT domains pack closely against each other in a head-to-tail manner burying a large hydrophobic interface and creating a deep surface groove. The CtIP peptide binds to this groove in a two-pronged mode, with phospho-Ser327 (pSer 0) and Phe330 (Phe +3) forming the main interactions with BRCT1 and BRCT2, respectively (Fig. 1, *A* and *B*), consistent with biochemical and functional studies on the importance of these residues for the BRCA1–CtIP association (16–19). The phosphate group of pSer 0 forms hydrogen bonds with the side chains of Ser1655 and Lys1702, the amide nitrogen of Gly1656, and the amide nitrogen of Lys1702 through a water-mediated interaction (Fig. 1*C*). The phenyl ring of Phe +3 is inserted in a hydrophobic pocket made up of the BRCT2 residues Leu1701, Phe1704, Arg1699, Asn1774, Met1775, Arg1835, and Leu1839, whereas the carbonyl oxygen and amide nitrogen of Phe +3 hydrogen bond with the N^ϵ and carbonyl oxygen of Arg1699, respectively (Fig. 1, *B* and *C*). To a lesser degree, the CtIP residues Val –2, Pro +1, and Gly +4 also contribute to the interaction though van der Waals contacts and water-mediated hydrogen bonds (Fig. 1*C*).

Structural Basis for Disruption of the BRCA1–CtIP Interaction by Cancer-associated Mutations—A number of missense mutations within the BRCT repeats abrogate the tumor suppression activity of BRCA1 and are associated with a high incidence of cancer but there have been difficulties in explaining how they exert their effects. In two such mutations, M1775R and R1699W, the affected BRCT residues participate in the formation of the hydrophobic pocket that

receives the Phe +3 phenyl ring of the BACH1 (21, 22, 24) and CtIP phosphopeptides (Fig. 1, *B* and *C*). The M1775R mutation inhibits the BRCA1 interaction with BACH1 (11, 17, 21, 22) and CtIP (13) and leads to defects in the DSB repair (32) and transactivation functions of BRCA1 (33). Superposition of the BRCA1–CtIP and the unbound mutant BRCT(M1775R) crystal structures (34) shows that the guanido group of the substituted Arg1775 sterically clashes with the phenyl ring of Phe +3, directly obstructing the insertion of this anchoring group into the pocket (Fig. 1*D*), as described for the effect of M1775R on the BRCA1–BACH1 interaction (21–24). In the case of R1699W, it is predicted that the hydrogen bond between the N^ϵ of Arg1699 and the carbonyl oxygen of Phe +3 will be lost and the large indole group of Trp1699 will likely occlude the entrance of the phenyl ring into the pocket.

Comparison of the BRCT–CtIP and BRCT–BACH1 Complexes—Superposition of the BRCA1–CtIP and BRCA1–BACH1 structures shows that the BRCT repeats and the backbones of five residues (pSer 0 to Gly +4) are superimposed well (root-mean-square deviation of 0.71 Å for all C^α atoms), whereas the N- and C-terminal portions of the peptides are not superimposable (Fig. 2*A*). The O^γ atom of the BACH1 Ser –2 hydrogen bonds to the amide nitrogen of Gly1656, whereas in the BRCT–CtIP complex the $C^{\gamma2}$ atom of the Val –2 isopropyl group makes hydrophobic contacts with Leu1657 and displaces the peptide backbone away from the BRCT groove (Fig. 1, *A* and *C*). Interestingly, the guanido group of the CtIP Arg –3 folds back and forms two hydrogen bonds with the carbonyl oxygen of Ser –1, further stabilizing the peptide orientation and preventing any additional N-terminal interactions. Notably, a similar interaction of Arg –3 has not been observed in any of the BRCA1–BACH1 structures (21, 22).

Additional differences in the interaction of the BRCTs with BACH1 and CtIP are observed at the C-terminal regions of the phosphopeptides. Whereas the side chain of BACH1 Asn +4 makes two water-mediated hydrogen bonds with the BRCT residues Glu1689 and Arg1699 (22), these bonds are missing in the BRCA1–CtIP structure because a glycine occupies the position +4 in CtIP (Fig. 1*C*). Likewise, the side chain of BACH1 Lys +5 makes salt bridges with Glu1863 and Asp1840

(22), while similar interactions are missing in the BRCA1–CtIP complex due to the presence of Ala +5 in CtIP. The fewer interactions observed in the association of the BRCA1 BRCT repeats with CtIP than those described for BACH1 suggest a weaker association of these domains with the former phosphopeptide.

The BRCA1 BRCT Domains Exhibit a Higher Affinity for BACH1 than CtIP—To determine the effects of these structural differences in the strength of the BRCA1–CtIP and BRCA1–BACH1 interactions, we measured the affinities of these complexes using isothermal titration calorimetry. The BRCA1 BRCT domains bind to the BACH1 phosphopeptide with a dissociation constant (K_d) of 0.7 μM (Fig. 2*B*), which is in good agreement with the reported K_d of 0.9 for a similar BACH1 peptide (21). By contrast, the BRCT repeats bind to the CtIP phosphopeptide with a K_d of 3.7 μM (Fig. 2*C*). The ~5-fold higher binding affinity of the BRCA1 BRCTs for BACH1 than CtIP can be attributed mainly to the hydrogen bonding network involving the BACH1 residues Ser –2, Asn +4, and Lys +5 that is missing in the BRCA1–CtIP complex. These findings support the conclusion that residues surrounding pSer 0 and Phe +3 make significant contributions to the BRCT–ligand interaction and account for the affinity differences of various binding partners for the BRCT modules. These differences determine both the dynamic target selection among competing proteins that have distinct roles in cell cycle checkpoints and DNA repair for binding to BRCA1 and the duration of these interactions. For example, the association of the BRCA1 BRCT repeats with BACH1 leads to a stable complex that accumulates in the G_2 and M phases of the cell cycle, whereas the lower affinity of these domains for CtIP generates a transient complex during the G_2 phase that controls the G_2/M transition checkpoint (16).

Structural and Functional Implications—In addition to BACH1 and CtIP, other potential binding targets for the BRCA1 BRCT repeats have been identified in database searches with their consensus binding motif (19), including BRCA1 itself, the DNA mismatch repair protein MSH3 (35), hTID1, the human homolog of the *Drosophila* tumor suppressor l(2)Tid that modulates apoptosis (36), the CCCTC-binding factor CTCF that functions as a chromatin insulator and transcription factor implicated in the regulation of *BRCA1* gene expression (37), and the nuclear receptor co-activator NCoA-3/AIB1 that is amplified in breast and ovarian cancer (38) and regulates the estrogen-mediated survival and proliferation of breast carcinoma cells (39). Structural and biophysical analyses of the BRCA1 BRCT domains bound to their targets, including CtIP, BACH1, and the aforementioned proteins, will elucidate the mechanisms underlying the dynamic interactions of these versatile modules with various proteins during cell cycle control, DNA repair, chromatin remodeling, and transcription regulation. Furthermore, these studies will provide a structural explanation for the detrimental effects of breast/ovarian cancer-linked BRCT missense mutations on BRCA1 function.

Importantly, the atomic structures of the BRCA1 BRCT domains bound to CtIP, BACH1 and other targets could be exploited for improving current radiation therapy protocols for cancer. Because DNA damage-induced cell cycle checkpoints confer radioresistance to tumor cells, it has been suggested that inhibition of the checkpoint and DNA repair processes could result in more effective cancer treatments (40). BRCA1 controls the G2/M checkpoint through interactions with BACH1 and CtIP (16) and induces a large increase in resistance to agents that generate DSBs (41), whereas BRCA1-deficient cells are hypersensitive to ionizing radiation and DNA cross-linking agents (9, 10, 32). It is therefore conceivable that the atomic models of the BRCA1 BRCT domains bound to CtIP, BACH1, and other targets could provide a structural framework for the design of small-molecule inhibitors of these interactions that would enhance the sensitivity of tumor cells to radiation therapy and chemotherapy.

4

REFERENCES

1. Narod, S. A., and Foulkes, W. D. (2004) *Nat. Rev. Cancer* **4,** 665-676
2. Rosen, E. M., Fan, S., Pestell, R. G., and Goldberg, I. D. (2003) *J. Cell. Physiol.* **196,** 19-41
3. Sancar, A., Lindsey-Boltz, L. A., Unsal-Kacmaz, K., and Linn, S. (2004) *Annu. Rev. Biochem.* **73,** 39-85
4. Vallon-Christersson, J., Cayanan, C., Haraldsson, K., Loman, N., Bergthorsson, J. T., Brondum-Nielsen, K., Gerdes, A. M., Moller, P., Kristoffersson, U., Olsson, H., Borg, A., and Monteiro, A. N. (2001) *Hum. Mol. Genet.* **10,** 353-360
5. Ludwig, T., Fisher, P., Ganesan, S., and Efstratiadis, A. (2001) *Genes Dev.* **15,** 1188-1193
6. Xu, B., Kim, S., and Kastan, M. B. (2001) *Mol. Cell. Biol.* **21,** 3445-3450
7. Moynahan, M. E., Chiu, J. W., Koller, B. H., and Jasin, M. (1999) *Mol. Cell* **4,** 511-518
8. Xu, X., Weaver, Z., Linke, S. P., Li, C., Gotay, J., Wang, X. W., Harris, C. C., Ried, T., and Deng, C. X. (1999) *Mol. Cell* **3,** 389-395
9. Bhattacharyya, A., Ear, U. S., Koller, B. H., Weichselbaum, R. R., and Bishop, D. K. (2000) *J. Biol. Chem.* **275,** 23899-23903
10. Moynahan, M. E., Cui, T. Y., and Jasin, M. (2001) *Cancer Res.* **61,** 4842-4850
11. Cantor, S. B., Bell, D. W., Ganesan, S., Kass, E. M., Drapkin, R., Grossman, S., Wahrer, D. C., Sgroi, D. C., Lane, W. S., Haber, D. A., and Livingston, D. M. (2001) *Cell* **105,** 149-160
12. Schaeper, U., Subramanian, T., Lim, L., Boyd, J. M., and Chinnadurai, G. (1998) *J. Biol. Chem.* **273,** 8549-8552
13. Yu, X., Wu, L. C., Bowcock, A. M., Aronheim, A., and Baer, R. (1998) *J. Biol. Chem.* **273,** 25388-25392
14. Wong, A. K., Ormonde, P. A., Pero, R., Chen, Y., Lian, L., Salada, G., Berry, S., Lawrence, Q., Dayananth, P., Ha, P., Tavtigian, S. V., Teng, D. H., and Bartel, P. L. (1998) *Oncogene* **17,** 2279-2285
15. Yu, X., and Baer, R. (2000) *J. Biol. Chem.* **275,** 18541-18549
16. Yu, X., and Chen, J. (2004) *Mol. Cell. Biol.* **24,** 9478-9486
17. Manke, I. A., Lowery, D. M., Nguyen, A., and Yaffe, M. B. (2003) *Science* **302,** 636-639
18. Yu, X., Chini, C. C., He, M., Mer, G., and Chen, J. (2003) *Science* **302,** 639-642
19. Rodriguez, M., Yu, X., Chen, J., and Songyang, Z. (2003) *J. Biol. Chem.* **278,** 52914-52918
20. Meloni, A. R., Smith, E. J., and Nevins, J. R. (1999) *Proc. Natl. Acad. Sci. USA* **96,** 9574-9579
21. Shiozaki, E. N., Gu, L., Yan, N., and Shi, Y. (2004) *Mol. Cell* **14,** 405-412
22. Clapperton, J. A., Manke, I. A., Lowery, D. M., Ho, T., Haire, L. F., Yaffe, M. B, and Smerdon, S. J. (2004) *Nat. Struct. Mol. Biol.* **11,** 512-518
23. Williams, R. S., Lee, M. S., Hau, D. D., and Glover, J. N. (2004) *Nat. Struct. Mol. Biol.* **11,** 519-525
24. Botuyan, M. V., Nomine, Y., Yu, X., Juranic, N., Macura, S., Chen, J., and Mer, G. (2004) *Structure* **12,** 1137-1146
25. Otwinowski, Z., and Minor, W. (1997) *Methods Enzymol.* **276,** 307-326
26. Storoni, L. C., McCoy, A. J., and Read, R. J. (2004) *Acta Crystallogr. Sec. D* **60,** 432-438
27. Collaborative Computational Project Number 4 (1994) *Acta Crystallogr. Sec. D* **50,** 760-763
28. Murshudov, G. N., Vagin A. A., and Dodson, E. J. (1997) *Acta Crystallogr. Sec. D* **53,** 240-255
29. Brunger, A. T., Adams, P. D., Clore, G. M., DeLano, W. L., Gros, P., Grosse-Kunstleve, R. W., Jiang, J. S., Kuszewski, J., Nilges, M., Pannu, N. S., Read, R. J., Rice, L. M., Simonson, T., and Warren, G. L. (1998) *Acta Crystallogr. Sec. D* **54,** 905-921
30. Jones, T. A., Zou, J. Y., Cowan, S., and Kjeldgaard, M. (1991) *Acta Crystallogr. Sec. A* **47,** 110-119
31. Perrakis, A., Morris, R., and Lamzin, V. S. (1999) *Nat. Struct. Biol.* **6,** 458-463
32. Scully, R., Ganesan, S., Vlasakova, K., Chen, J., Socolovsky, M., and Livingston, D. M. (1999) *Mol. Cell* **4,** 1093-1099
33. Monteiro, A. N., August, A., and Hanafusa, H. (1996) *Proc. Natl. Acad. Sci. USA* **93,** 13595-13599
34. Williams, R. S., and Glover, J. N. (2003) *J. Biol. Chem.* **278,** 2630-2635

3

35. Kleczkowska, H. E., Marra, G., Lettieri, T., and Jiricny, J. (2001) *Genes Dev.* **15,** 724-736
36. Syken, J., De-Medina, T., and Munger, K. (1999) *Proc. Natl. Acad. Sci. USA* **96,** 8499-8504
37. Butcher, D. T., Mancini-DiNardo, D. N., Archer, T. K., and Rodenhiser, D. I. (2004) *Int. J. Cancer* **111,** 669-678
38. Anzick, S. L., Kononen, J., Walker, R. L., Azorsa, D. O., Tanner, M. M., Guan, X. Y., Sauter, G., Kallioniemi, O. P., Trent, J. M., and Meltzer, P. S. (1997) *Science* **277,** 965-968
39. Weldon, C. B., Elliott, S., Zhu, Y., Clayton, J. L., Curiel, T. J., Jaffe, B. M., and Burow, M. E. (2004) *Surgery* **136,** 346-354
40. Hartwell, L. H., and Kastan, M. B. (1994) *Science* **266,** 1821-1828
41. Quinn, J. E., Kennedy, R. D., Mullan, P. B., Gilmore, P. M., Carty, M., Johnston, P. G, and Harkin, D. P. (2003) *Cancer Res.* **63,** 6221-6228
42. Wallace, A. C., Laskowski, R. A., and Thornton, J. M. (1995) *Protein Eng.* **8,** 127-134
43. Nicholls, A., Sharp, K. A., and Honig, B. (1991) *Proteins* **11,** 281-296

FOOTNOTES

The atomic coordinates and structure factors (code 1Y98) have been deposited in the Protein Data Bank, Research Collaboratory for Structural Bioinformatics, Rutgers University, New Brunswick, NJ (http://www.rcsb.org/).

[1] The abbreviations used are: BACH1, BRCA1-associated C-terminal helicase; BRCA1, breast and ovarian cancer susceptibility gene 1; BRCT, BRCA1 C-terminal; CtIP, CtBP-interacting protein.

FIGURE LEGENDS

FIG. 1. **CtIP recognition by BRCA1 BRCT domains.** *A*, ribbons representation of the BRCA1 BRCTs bound to the CtIP peptide (*cyan* stick model). The α-helices and β-strands are colored *yellow* and *green*, respectively. The BRCT2 secondary structure elements are labeled with *primes*. The BRCT linker helix αL is colored *orange*. The critical residues pSer 0 and Phe +3 are denoted. The figure was made using PyMOL (www.pymol.org) and POV-Ray (www.povray.org). *B*, a $2F_o - F_c$ electron density map at the Phe +3 binding site calculated at 2.5 Å resolution and contoured at 1.0 σ. *C*, two-dimensional representation of the interactions between BRCA1 (*orange*) and CtIP (*purple*) residues. Water molecules (W) are shown as *cyan spheres*, hydrogen bonds as *dashed lines*, and hydrophobic interactions as *arcs* with *radial spokes*. The figure was made using LIGPLOT (42). *D*, superposition of the BRCT–CtIP and BRCT(M1775R) mutant (PDB 1N5O) crystal structures shows the steric hinderance between the Arg1775 (*pink*) and Phe +3 (*cyan*) side chains. The figure was made with GRASP (43).

FIG. 2. **Comparison of the BRCA1–BACH1 and BRCA1–CtIP interactions.** *A*, superposition of the crystal structures of the BRCA1 BRCTs (*beige*) bound to the BACH1 peptide (*blue* stick model) (PDB 1T29) and the BRCTs (*green*) bound to CtIP (*orange* stick model). *B* and *C*, representative isothermal titration calorimetry results obtained for the BRCA1 BRCT interaction with the BACH1 and CtIP phosphopeptides, respectively.

TABLE 1

Statistics of structure determination and refinement

Resolution range (Å)	20 – 2.5
Observed reflections	179,377
Unique reflections	16,294
Completeness (%)[a]	99.1 (99.4)
R_{sym} (%)[b]	13.3 (37.2)
Overall $<I/\sigma(I)>$	17.5 (2.7)
R_{cryst} (%)[c]	23.4
R_{free} (%)[d]	26.9
Ramachandran plot (%)	
Most favored region	79.0
Allowed region	18.5
Generously allowed	2.6
Bond lengths[e] (Å)	0.016
Bond angles[e] (degrees)	1.78

[a] Values in parentheses are for the highest resolution shell (2.59 – 2.50 Å).

[b] $R_{sym} = \Sigma |(I - <I>)|/\Sigma(I)$, where I is the observed integrated intensity, $<I>$ is the average integrated intensity obtained from multiple measurements, and the summation is over all observed reflections.

[c] $R_{cryst} = \Sigma ||F_{obs}| - k|F_{calc}||/\Sigma|F_{obs}|$, where F_{obs} and F_{calc} are the observed and calculated structure factors, respectively.

[d] R_{free} is calculated as R_{cryst} using 6.25% of the reflections chosen randomly and omitted from the refinement calculations.

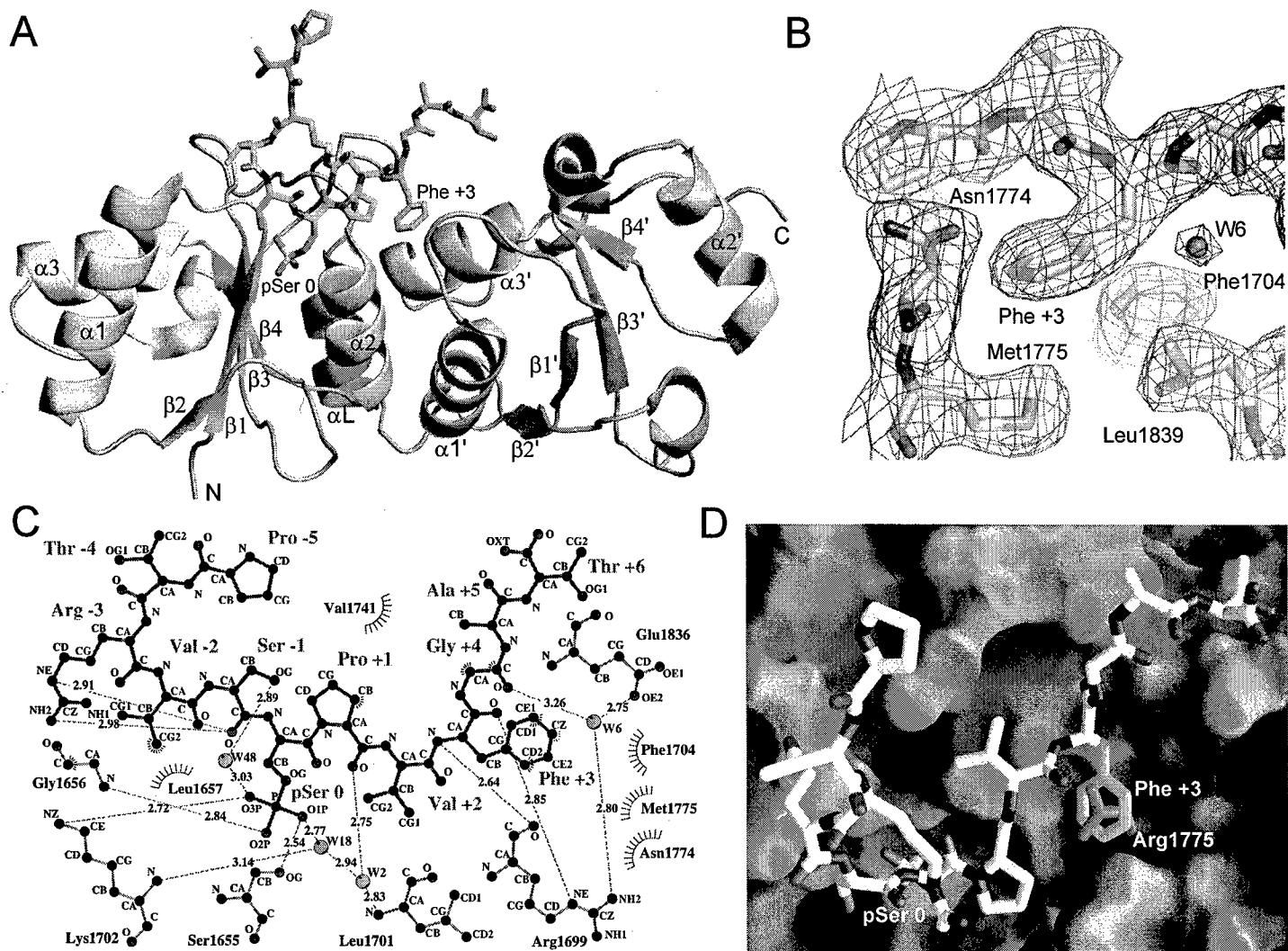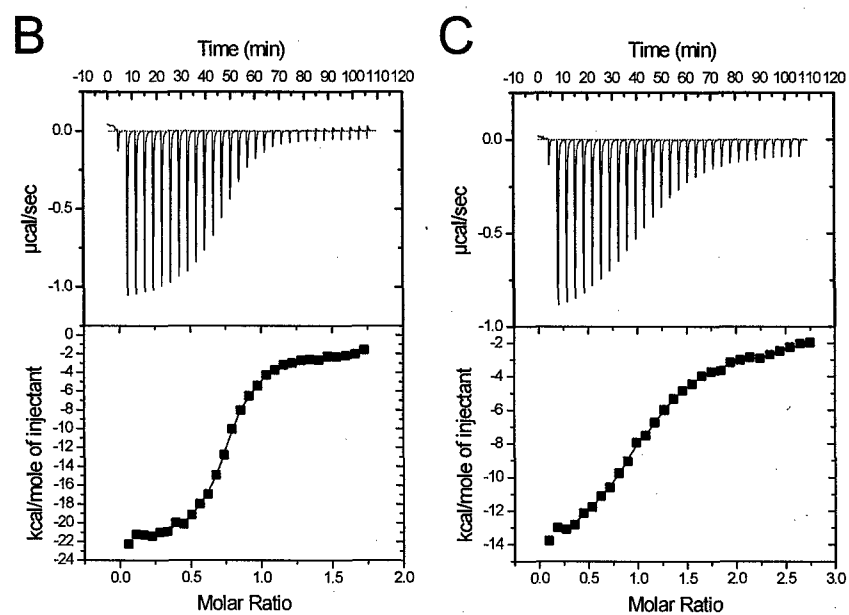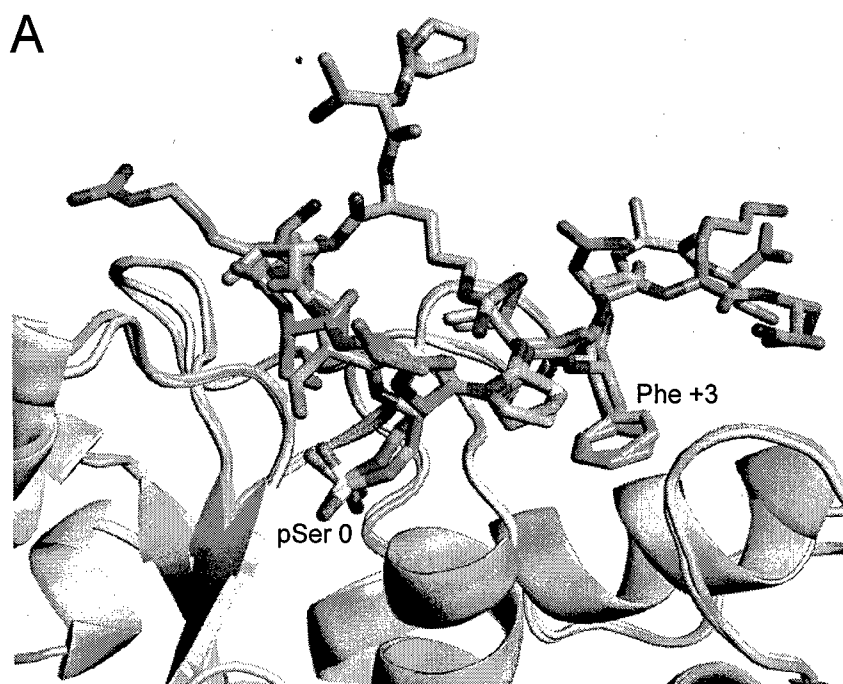[e] Bond lengths and angles are root-mean-square deviations from ideal values.

Figure 1

Figure 2